Trap-loss collisions of ^{85}Rb and ^{87}Rb: Dependence on trap parameters

S. D. Gensemer, V. Sanchez-Villicana,* K. Y. N. Tan, T. T. Grove,† and P. L. Gould
Department of Physics, U-46, University of Connecticut, Storrs, Connecticut 06269-3046
(Received 21 March 1997)

We report on measurements of trap-loss collisions between ultracold Rb atoms that are confined in a magneto-optical trap. Both isotopes, ^{85}Rb and ^{87}Rb, have been studied over a wide range of trap laser intensities and detunings. The trap-loss collisional rate constant exhibits variations over three orders of magnitude. At low intensities and/or large detunings, the trap loss is dominated by ground-state hyperfine-changing collisions, while at high intensities and small detunings, collisions involving excited atoms are more important. We see significant differences between the isotopes in both regimes. At large detunings, the ability of the trap to recapture products of a hyperfine-changing collision is significantly diminished. This finding is supported by our numerical simulations of the recapture process. The trap loss rates due to collisions with room-temperature background gas have also been measured. A surprisingly large increase in this rate is seen when the confining power of the trap is reduced. [S1050-2947(97)10011-7]

PACS number(s): 32.80.Pj, 34.50.Rk

I. INTRODUCTION

Collisions between laser-cooled atoms have become an important area of investigation in atomic and molecular physics [1–6]. At submillikelvin temperatures, long-range potentials dominate the collision dynamics. This fact, coupled with the low collision velocities, results in greatly increased time and length scales for the collisions. The intense interest in these ultracold collisions stems not only from these novel features, but also from their importance in applications of laser-cooled atoms (e.g., atomic clocks and Bose-Einstein condensation). Since most of these applications require high densities and low temperatures, collisional interactions between the cold atoms can be a limiting mechanism. Hence, a thorough understanding of these processes is important.

In this work, we concentrate on trap-loss collisions (TLC), i.e., collisions that lead to ejection from the magneto-optical trap that confines the atoms. We also restrict ourselves to collisions that occur under the influence of the trap environment. We do not consider collisions induced by a separate laser. Such ''catalysis'' laser experiments [7–12] provide much useful information, especially for relatively large detunings from the atomic resonance. However, they do not yield insight into collisions that are important for typical operating conditions of laser traps. Collisions due to the trap itself are more difficult to understand fully because many relevant parameters (e.g., temperature, excited-state fraction, trap depth) change as the trap parameters are varied. On the other hand, careful investigations can yield information not only about the collisions themselves, but also about properties of the trap. As an example, in the present work we show that for our conditions, the confining power of the trap degrades rapidly as the trap detuning is increased.

Previous work has investigated TLC in various atomic systems: Li [13–15], Na [16–18], K [19], Rb [20,21], and Cs [7]. For atoms with relatively large ground-state hyperfine splittings (Na,Rb,Cs), the following behavior has been observed. At low trap laser intensities, the trap is sufficiently weak that inelastic ground-state hyperfine-changing (ΔF) collisions can result in the ejection of both colliding atoms from the trap. As the trap intensity is increased, the trap becomes deep enough to retain these atoms and the TLC rate goes down. At the same time, the higher intensity causes a greater atomic excitation, which in turn results in an increased trap-loss rate due to collisions involving excited-state atoms. These inelastic collisions are due to either a fine-structure change (ΔJ) in the excited atom or radiative escape (RE) in which the excited atom pair emits a less energetic photon (at short range) than it absorbed (at long range), converting the difference into kinetic energy. Because of these ground-excited collisions, the TLC rate reaches a minimum when the ΔF loss channel is turned off and starts to rise again as the intensity is increased. The case of Li [13–15] is somewhat unique because of the relatively small energy associated with a ΔJ collision. This ΔJ loss channel is similar to the ΔF channel in the heavier alkalis in that it can be turned off by making a deep enough trap. In K, the ground-state hyperfine splitting is so small that ΔF collisions would be difficult to observe.

In atoms with more than one available isotope, significant isotopic differences have been observed. In ^{85}Rb and ^{87}Rb [20], the TLC rates exhibit a dramatic isotopic dependence at both low intensities, where ΔF collisions dominate, and at higher intensities, where ground-excited collisions are more important. These findings have been explained in terms of the different hyperfine structures of the ground and excited states, respectively. Striking isotopic differences in ground-excited TLC have also been seen in ^{6}Li and ^{7}Li [22] and ^{39}K and ^{41}K [19].

Most experiments employ a magneto-optical trap [23] (MOT) operating close to resonance (within one or two natural linewidths) because this optimizes the capture efficiency [24]. Therefore, most collisional investigations, with the ex-

*Present address: Instituto Nacional de Astrofisica, Optica y Electronica, Tonanzintla, Puebla 72840, Mexico.

†Present address: Rome Laboratory, Hanscom Air Force Base, Bedford, MA 01731.

ceptions of Li [14,15] and K [19], have been restricted to this regime of small detunings. However, larger detunings are of interest because a reduced spontaneous emission rate can result in lower temperatures and higher densities [25,26]. In this work, we present results for TLC for both isotopes of Rb (^{85}Rb and ^{87}Rb) over a wide range of trap laser intensities and detunings. This extends our previous work to larger detunings and shows that the confining power of the trap, as measured by its ability to recapture products of a ΔF collision, degrades rather quickly as the detuning is increased. We are also able to gain some information on the rate of ground-excited collisions under different trap conditions. This paper is organized as follows. In Sec. II, we describe the experiment. In Sec. III, the measurements of the TLC rates are presented. Numerical simulations of the trap confining power and their comparison to experiment are discussed in Sec. IV. In Sec. V, we present and discuss the trap loss rates due to background gas collisions. Section VI is a summary.

II. EXPERIMENT

The trap-loss collisional rate constant β is measured by monitoring the time evolution of the number of trapped atoms [20]. Inelastic collisions between trapped atoms at a density n lead to ejection from the trap at a rate (per atom) of βn. In addition, cold atoms are lost from the trap at a rate (per atom) of γ due to collisions with room-temperature background gas. A measurement consists of loading the trap with an initial number of atoms, turning off the loading, and measuring the temporal decay of the trapped sample. Careful fitting of this decay curve, coupled with measurements of the absolute atomic density, yields the quantities β and γ.

The trap is a magneto-optical trap [23] realized by intersecting three orthogonal pairs of counterpropagating laser beams at the center of a quadrupole magnetic field. This magnetic field is produced by oppositely directed currents in a pair of parallel coils that are situated symmetrically about the trap center. For all the measurements reported here, the axial field gradient is set to 4.8 G/cm, resulting in a radial gradient of 2.4 G/cm. Additional sets of coils allow the Earth's magnetic field to be nulled. The trap laser beams are derived from a linewidth-narrowed and frequency-stabilized diode laser [27]. The laser light is transported through a polarization-maintaining single-mode optical fiber in order to spatially filter the light and ensure alignment stability. Three equal-intensity beams are derived from the fiber output and retroreflected to produce the MOT. Each pair is oppositely circularly polarized ($\sigma^+ - \sigma^-$). Antireflection coatings are used on all optics and windows in order to ensure balanced intensities and a trap that forms at the magnetic field zero. The trap beams are Gaussian with a $1/e^2$ diameter of 6.3 mm. Total trap intensities (sum of all six beams at the trap center) up to $I \approx 40$ mW/cm^2 are used. The trap laser detuning Δ, measured relative to the 780-nm $5S_{1/2}$ ($F = F_{\max}$)$\rightarrow 5P_{3/2}$ ($F' = F'_{\max}$) cycling transition, is varied between -1.0Γ and -4.0Γ ($\Gamma/2\pi = 5.9$ MHz is the full width at half maximum natural linewidth). For ^{85}Rb, $F_{\max}=3$ and $F'_{\max}=4$, while for ^{87}Rb, $F_{\max}=2$ and $F'_{\max}=3$.

A separate free-running diode laser (linewidth$\approx$30 MHz) overlaps the trap region and prevents optical pumping into the lower hyperfine level of the ground state. Its intensity is fixed at $\gtrsim 10$ mW/cm^2 and its frequency is modulated by $\sim$40 MHz at a rate of 1.6 kHz in order to facilitate long-term frequency stabilization.

The trap is situated in a UHV environment ($P \approx 10^{-10}$ torr) and loaded with an atomic Rb beam that is slowed by counterpropagating and frequency-chirped diode laser light. We operate at sufficiently low trapped atom densities that radiation trapping effects [28] are negligible, resulting in a constant volume throughout the decay. The maximum initial density (number) of trapped atoms used is typically 3×10^9 cm^{-3} (5×10^3) for a trap detuning $\Delta = -1\Gamma$ and intensity $I \approx 40$ mW/cm^2. At larger detunings and lower intensities (e.g., $\Delta = -4\Gamma$ and $I \approx 5$ mW/cm^2), the smaller excited-state fraction allows larger densities (e.g., 10^{10} cm^{-3}) and numbers (e.g., 5×10^4) to be used before radiative repulsion becomes significant. For measurements involving a weak trap (i.e., large detuning and low intensity), it is neccessary to use an additional overlapping trap (formed with a separate laser) to assist in the initial loading of the trap.

Determinations of the TLC rate constant β require measurements of the absolute atomic density. The number of trapped atoms is measured by combining the signal from a calibrated fluorescence collection and detection (PMT) system with the atomic excited-state fraction determined by photoionization [29]. The effective volume of the trapped cloud is determined by analyzing the image obtained with a charge-coupled device (CCD) camera. The clouds are Gaussian in shape with $1/e$ diameters ranging from 120 to 260 μm. Relative values of β can be considered accurate at the 20% level, as limited by uncertainties in trap volume. However, absolute values of β are only known to within a factor of $\sim$2, due to uncertainties in the atomic number calibration.

III. TRAP-LOSS COLLISION MEASUREMENTS

Measurements of the TLC rate constant for both isotopes (^{85}Rb and ^{87}Rb) are shown as a function of trap laser intensity, and for several different trap laser detunings, in Fig. 1. The most striking feature is the tremendous variation (over three orders of magnitude) in β. We will first discuss the data for smaller detunings: $\Delta = -1\Gamma, -2\Gamma$. The general trend is a large loss rate at low intensities, which decreases rapidly as the intensity is increased. We interpret this behavior as follows. At low intensity, the atoms are predominantly in the ground state (upper hyperfine level) and the effective trap depth is very small. Thus the trap loss rate is dominated by inelastic ground-state hyperfine-changing (ΔF) collisions. The energy (velocity) gained by each ^{85}Rb atom in such a collision is 73 mK (3.78 m/s) if only one atom changes its value of F (denoted $1\times\Delta F$), and 146 mK (5.34 m/s) if both atoms change their value of F (denoted $2\times\Delta F$). The corresponding values for ^{87}Rb are 164 mK (5.60 m/s) for $1\times\Delta F$ and 328 mK (7.92 m/s) for $2\times\Delta F$. As noted previously [20] (for a detuning of $\sim -1\Gamma$), this difference in the ground-state hyperfine structure between ^{85}Rb and ^{87}Rb is responsible for the isotopic variation in β at low intensities. In the present data, we see that the sharp decrease in β occurs at a lower intensity for ^{85}Rb than for ^{87}Rb (for both $\Delta = -1\Gamma$ and -2Γ), indicative of the smaller energy associated with the ^{85}Rb ΔF collisions. Another obvious feature is

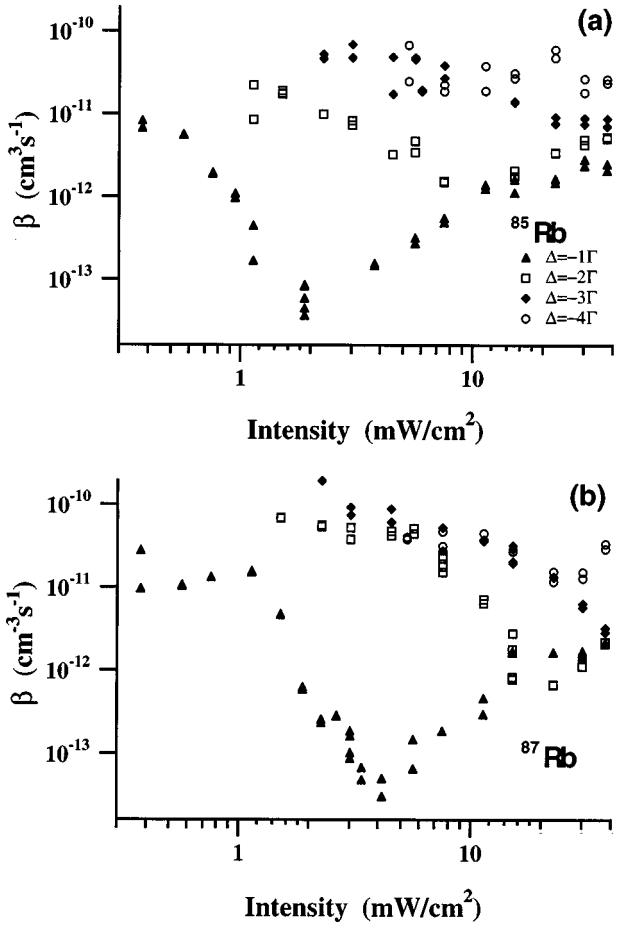

FIG. 1. Trap loss collisional rate β vs total trap laser intensity for (a) ^{85}Rb and (b) ^{87}Rb. Different trap detunings are denoted by different symbols. The axial magnetic field gradient is 4.8 G/cm and the beam size is 6.3 mm ($1/e^2$ diameter).

that, for each isotope, the sharp decrease in β occurs at a significantly higher intensity for $\Delta=-2\Gamma$ than for $\Delta=-1\Gamma$. This demonstrates that, for a given intensity, the trap depth is significantly less for $\Delta=-2\Gamma$ than for $\Delta=-1\Gamma$. As we will see in Sec. IV, this is supported by our numerical simulations of the trap-loss process.

Further evidence that the high values of β at low trap intensities are due to ΔF collisions is obtained by looking at the effect of the repumping laser. Obviously, after a ΔF collision, at least one of the atoms ends up in the lower hyperfine level. In order for the trap to recapture this atom, it must first be optically pumped back into the upper hyperfine level. The longer this repumping takes, the further this fast atom will move before feeling the force of the trap laser; e.g., if repumping takes 100 μs following a ^{87}Rb $2\times\Delta F$ collision, the atom will travel ~0.8 mm away from the trap center without experiencing any opposing force. Since the $1/e^2$ radius of the trap beams is only ~3.2 mm, this free flight will significantly facilitate the atom's escape. In the experiment, we can lengthen the repumping time by attenuating the repumping laser. Setting the trap laser detuning at $\Delta=-1\Gamma$ and $I=2$ mW/cm^{-2} for ^{87}Rb [i.e., on the sharply decreasing region of the curve in Fig. 1(b)], we look for a change in β as we reduce the intensity of the repumping laser. We see no effect for attenuations up to a factor of 4, at which point β increases sharply. This indicates that at least one of the colliding atoms ends up in the lower hyperfine level. We note that properties of the trapped sample itself (e.g., volume, excited-state fraction) are unchanged for attenuations up to a factor of 10. This is to be expected because optical pumping into the lower hyperfine level (by the trap laser) is very slow due to the large excited-state hyperfine splittings of Rb.

After its sharp decrease, β reaches a minimum and then starts to increase with intensity. The behavior in this regime is complicated by a combination of several factors. As we increase the trap laser intensity, the number of excited atoms, and therefore the rate of ground-excited collisions, goes up. However, properties of the trap also change. First, the temperature of the trapped atoms rises with increasing intensity [30]. In certain regimes (low temperature and small detuning), we have seen [21] a suppression of the ground-excited collisional loss rate as the temperature is lowered. This is because, at low collision velocities, the atomic excitation is more likely to decay during the joumey from long range (where it is created) to short range (where the inelastic process occurs). Second, the trap gets deeper (i.e., it is able to confine more energetic atoms) as we go to higher intensity. This latter factor is only important for RE because these collisions impart a wide range of energies to the atoms. For a given trap depth, only those atoms gaining an energy greater than that depth will escape. All others will be recaptured. Therefore, as the trap depth increases, a smaller fraction of RE collisions will result in trap loss. More specifically, the trap loss rate is predicted [2] to scale with trap depth U as $U^{-5/6}$. This is not an issue for ΔJ collisions because they impart a well-defined energy (171 K) per atom that is large compared to typical trap depths (~1 K). Based on the simultaneous variation of excitation (with possible saturation), temperature, and trap depth with trap laser intensity, and uncertainties in the relative importance of RE and ΔJ collisions, it is difficult to interpret the collisional trap-loss rate caused by trap laser excitation.

At a detuning $\Delta=-1\Gamma$, the general intensity dependence of β for both isotopes is a relatively rapid increase over the intensity range I_m to $\sim 4I_m$, where $I_m\sim 2$ mW/cm^2 (~ 4 mW/cm^2) is the intensity at which β has its minimum value for ^{85}Rb (^{87}Rb). We attribute this to the low-temperature suppression effect [21] discussed above. Note that in the range around $I=10$ mW/cm^2, we see the isotopic difference previously observed [20], i.e., β for ^{85}Rb is larger than that for ^{87}Rb by a factor of ~3. At higher intensities (i.e., above ~15 mW/cm^2), β becomes relatively independent of both intensity and isotope, assuming a value of $\sim 2\times 10^{-12}$ cm^{-3} s^{-1}. We do not have an explanation for this behavior. As discussed above, the detuning and intensity dependences are not easily interpreted in this regime because the trap laser is not only causing the collisions, but also determining the properties of the trapped sample and whether or not collision products escape.

For a detuning of $\Delta=-2\Gamma$, we do not see a pronounced minimum in β as we do for $\Delta=-1\Gamma$. The ΔF collisions dominate β out to much higher intensities due to the reduced confining power of the trap at this larger detuning. After its initial decrease (i.e., at intensities above that neccessary for complete recapture of ΔF collision products), β appears to rise slowly, taking on values similar to those for $\Delta=-1\Gamma$ in this regime. We note that the curves for the two isotopes

appear to cross as they do for $\Delta=-1\Gamma$. At low intensities, where ΔF collisions dominate, $\beta_{87}>\beta_{85}$, while at higher intensities, ground-excited collisions are the major contributor and $\beta_{87}<\beta_{85}$. The latter situation is consistent with previous findings that $\beta_{87}<\beta_{85}$ for ground-excited collisions induced by a separate laser [9,10] detuned by less than the excited-state hyperfine splitting. This behavior has been explained in terms of the effects of the isotopic difference in the excited-state hyperfine structure [31,12].

At the larger detunings ($\Delta=-3\Gamma$ and -4Γ), the trap-loss rates are very high for both isotopes over almost the entire range of intensities. We attribute this to the rapid deterioration of the trap's ability to recapture products of a ΔF collision as the detuning is increased. This is supported by the simulations discussed in the following section. For $\Delta=-3\Gamma$, the data do show a decrease of β with increasing intensity at the highest intensities. Once again, the curves for the two isotopes appear to cross as they do for $\Delta=-1\Gamma$ and -2Γ.

We have strong additional evidence, based on the effects of superimposing another MOT, that the large values of β at the larger detunings are primarily due to ΔF collisions. First, we measure β for ^{85}Rb at $\Delta=-4\Gamma$ and $I=30$ mW/cm^2. Then we superimpose another MOT with $\Delta=-1\Gamma$ and $I=2$ mW/cm^2 and measure β again. This second MOT is capable of recapturing products of a ΔF collision [see Fig. 1(a)], so we would expect β to be reduced significantly when it is present. This is exactly what we observe. The second MOT reduces β by $\sim$80%, indicating that the majority of the trap-loss collisions result in low-energy products that are recaptured by the second MOT. The residual β may be due to ground-excited collisions caused by the $\Delta=-4\Gamma$ MOT.

One trend of the complete data set is somewhat surprising. For a given detuning, we would expect the values of β at the lowest intensities (where the excited-state fraction is very low) to be limited by the total rate of ground-state ΔF collisions (recall that β is the collisional *loss* rate, not the collisional rate). Such a plateau, corresponding to a 100% escape rate for ΔF collisions, is indeed seen in the data. It is especially clear for ^{87}Rb. However, the level of this plateau seems to increase significantly as we go to larger detunings. This is rather unexpected since the rate of ground-state collisions should be independent of detuning. One possible explanation is that the trap laser enhances the flux available for these ground-state collisions. Such an enhancement has recently been observed for ground-excited collisions in Rb [32].

IV. NUMERICAL SIMULATIONS OF THE TRAP RECAPTURE PROCESS

As discussed in the preceding section, the ability of the trap to recapture products of a ΔF collision depends critically on the intensity and detuning of the trap laser. In general, the radiative forces acting on an atom in a MOT are dependent on both the atomic velocity (via the Doppler shift) and the atomic position (via the Zeeman shift). The former dependence gives rise to a damping force (for small velocities) while the latter results in a restoring force (for small displacements). The actual forces are rather complicated due to the three-dimensional aspects of the light field (i.e., pairs of counterpropagating and oppositely circularly polarized beams along x, y, and z), the Gaussian intensity profiles of the laser beams, the spatially dependent magnetic field, the multistate nature of the atom, and the nonlinear dependence of the force on velocity (for fast atoms) and position (for large displacements). Therefore, we have performed numerical simulations that take these various factors into account. These simulations are similar to those used recently to examine the roles of ΔJ and RE collisions in Li [15].

To simulate an inelastic collision, an atom is released from the center of the trap with an initial speed and direction. The radiative forces are then allowed to act on the atom and the trajectory is followed to determine whether it escapes. We include the quadrupole nature of the magnetic field, characterized by an axial field gradient $b=\partial B_z/\partial z$ (typically 4.8 G/cm). We also account for the Gaussian intensity profiles of the 6 laser beams, characterized by their $1/e^2$ diameter $2w_0$ (typically 6.5 mm). The trap laser is near resonance with the $5S_{1/2}(F=F_{\max})\rightarrow 5P_{3/2}(F'=F'_{\max})$ cycling transition and quite far from resonance with any other transitions, resulting in negligible excitation to levels other than $F'_{\max}$ (and subsequent optical pumping into $F\neq F_{\max}$). Since optical pumping is unlikely (and quickly corrected by the repumping laser), the simulation is restricted to the cycling transition.

The simulations utilize rate equations to calculate the local steady-state populations of the various magnetic sublevels m_F and $m_{F'}$. The quantization axis is taken to be the direction of the local magnetic field. Each laser beam is then decomposed into σ^+, σ^-, and π components relative to this axis and the excitation rates for each $m_F\rightarrow m_{F'}$ transition from each beam are calculated, accounting for the strength and Zeeman shift for each transition, and the Doppler shift for each beam. Saturation is included by accounting for the total stimulated rate (absorption and stimulated emission) due to all 6 beams. The steady-state solution of the rate equations (including absorption, stimulated emission, and spontaneous emission) gives the sublevel populations at that location. The force from a given beam is then calculated as the net absorption (absorption minus stimulated emission) rate from that beam times the momentum per photon. Note that this force is a time-averaged value and does not include the relatively small fluctuations caused by spontaneous emission. Also, our Doppler cooling treatment ignores wavelength-scale polarization gradients that are responsible for sub-Doppler cooling mechanisms [33,34]. At the relatively high initial velocities corresponding to ΔF collisions, Doppler cooling will dominate over sub-Doppler cooling. It is this Doppler force at high velocity that plays the major role in determining whether the atom escapes or is recaptured.

The simulations proceed by fixing the parameters of the trap, and following a large number of trajectories (e.g., 1000) that have a fixed initial speed (corresponding to a ΔF collision) and are uniformly distributed in their initial direction. This determines the escape fraction. The averaging over direction is very important because of anisotropies in the magnetic field (i.e., the axial gradient is twice the radial gradient) and the fact that the incident radiation is not spherically symmetric. This latter fact, coupled with the nonlinear dependence of the force on velocity, causes the magnitude of the radiative force to depend on the direction of motion as well as the speed. Results of these simulations are shown in Fig.

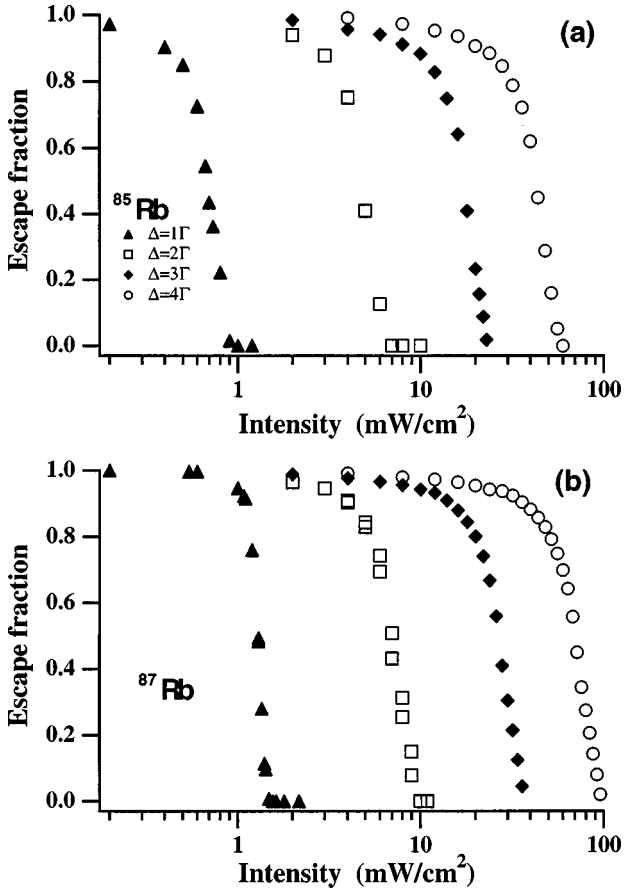

FIG. 2. Fraction of atoms escaping from the MOT as a function of total trap laser intensity for (a) ^{85}Rb and (b) ^{87}Rb. The three-dimensional numerical simulations assume initial velocities corresponding to $2\times\Delta F$ collisions: $v=5.34$ m/s for ^{85}Rb and 7.92 m/s for ^{87}Rb. Different trap detunings are denoted by different symbols. The axial field gradient is 4.8 G/cm and the beam size is 6.5 mm ($1/e^2$ diameter).

2. Parameters are chosen to correspond to the experiment (assuming $2\times\Delta F$ collisions) and the escape fraction is plotted as a function of trap laser intensity for different detunings. Several features are immediately obvious. First, for a given detuning, the anisotropy of the trap manifests itself in the finite slope of the curve. If the trap were isotropic, with a single, well-defined trap depth, the escape fraction would drop suddenly from 1 to 0 when this trap depth matched the fixed energy gained in the collision. The magnetic field anisotropy is verified to contribute to the trap depth anisotropy by performing one-dimensional trap depth calculations (discussed later in this section) for different magnetic-field gradients. Second, we see that for our relatively small beams, the ability of the trap to recapture products of a $2\times\Delta F$ collision degrades rapidly as we go to larger detunings, i.e., at larger detunings, a larger intensity is required for recapture. Finally, in comparing the two isotopes, we see that for a given detuning, ^{87}Rb requires a higher intensity for recapture than does ^{85}Rb. This is due to the larger ground-state hyperfine splitting, and therefore higher initial velocity, of ^{87}Rb. Our simulations indicate that for a given initial energy, the ability of the trap to recapture the two isotopes is similar.

Comparing the simulations (Fig. 2) to the data (Fig. 1), we see that the three features discussed above (anisotropy, detuning dependence, and isotopic dependence) are common to both. In order to make quantitative comparisons, we find the values of trap intensity neccessary to recapture 90% of the escaping atoms. According to this criterion, the trap depth is defined by the energy that results in a 10% (directionally averaged) escape fraction. From the data, this critical intensity I_c is determined (for a given isotope and detuning) by first finding the maximum value of β at low intensity (i.e., the low intensity plateau). I_c is then the intensity at which β has fallen to 10% of its maximum value. Values of I_c resulting from the experiment and from the simulations are compared in Table I. Uncertainties in the experimental values are due to uncertainties in the level of the plateau as well as the overall scatter in the measurements. There is also a ~15% calibration uncertainty in the measured intensity. Overall, the quantitative agreement is seen to be reasonable. The simulations tend to underestimate the experimental values of I_c to some degree. The measured detuning dependence of I_c is matched quite well with that from the simulations, verifying the rapid deterioration of the confining power of the trap at larger detunings. The isotopic difference is also in reasonable agreement with the measurements. For a given detuning, the ratio of $I_c(^{87}\mathrm{Rb})$ to $I_c(^{85}\mathrm{Rb})$ is seen to be ~1.6 in both the simulations and the measurements. The measured values for $\Delta=-3\Gamma$, however, do not seem to follow this trend. Finally, we note that $2\times\Delta F$ collisions were assumed in the simulations shown in Fig. 2. If $1\times\Delta F$ collisions were assumed instead, the values of I_c would be significantly lower, making them somewhat inconsistent with the measured values. Although we cannot rule out contributions from both types of collisions, our comparisons between data and simulations do indicate a significant presence of $2\times\Delta F$ collisions. This is consistent with recent measurements of trap depth (using repulsive trap-loss collisions), which demonstrate that for conditions where β_{85} is minimized [see Fig. 1(a)], the trap is sufficiently deep to confine products of a $2\times\Delta F$ collision [35].

TABLE I. Comparisons of measured and simulated critical intensities I_c (in mW/cm^2), defined according to 10% escape fraction, for various detunings and for the two isotopes. Blank entries were unable to be determined from the data.

Detuning	I_c (Simulations)	I_c (Experiment)
^{85}Rb		
-1Γ	0.86	0.99±0.1
-2Γ	6.1	7.3±1.5
-3Γ	21.8	26.9±5
-4Γ	54.2	
^{87}Rb		
-1Γ	1.4	1.7±0.2
-2Γ	8.9	11.2±1
-3Γ	34.6	27.3±5
-4Γ	90.7	

An important result that emerges from these simulations is that under our conditions of relatively small laser beams and magnetic-field gradients, the velocity-dependent damping forces ($-\alpha v$) and the position-dependent restoring forces ($-kz$) both play a role in preventing the escape of an

atom. The relative importance of these two forces changes throughout the trajectory. At the beginning, the atom has a large velocity and is located near the trap center. Obviously, the damping force dominates here. Away from the trap center, the velocity (and thus the damping force) is reduced, while the Zeeman shift (and thus the restoring force) is increased. In the Doppler cooling picture, the force as a function of velocity is linear near zero with a slope $(-\alpha)$ that is proportional to intensity. The force maximizes when the Doppler shift matches the detuning, and then decreases for higher velocity. If we have a fixed distance $z_{\max}$ to stop the atom (determined by the laser beam size) and the velocity is restricted to the region where the force is linear, the trap depth is given by $U=(\alpha^2 z_{\max}^2)/2m$, where m is the atomic mass. Since α is proportional to intensity (for intensities low enough that saturation is not important), we see that the trap depth should be proportional to the square of the intensity. This is in contrast to the case where position dependence dominates. Then $U=(kz_{\max}^2)/2$, and since k is proportional to intensity (again ignoring saturation), we would expect a trap depth proportional to intensity. We have performed simulations where we fix the intensity and vary the initial velocity in order to determine the trap depth (defined by 10% escape fraction). Plotting the trap depth as a function of intensity in Fig. 3(a), we see a power-law dependence for low intensities with an exponent between ~ 1.6 (for $\Delta=-1\Gamma$) and ~ 1.4 (for $\Delta=-4\Gamma$). These values are obviously between 1.0, expected for a pure restoring force, and 2.0, expected for a pure damping force. At the higher intensities (i.e., larger trap depths and therefore higher initial velocities), the slope is reduced by a combination of saturation and the deviation from linearity of the velocity-dependent force. To further demonstrate the importance of the restoring force, we have decreased the axial magnetic field gradient from 4.8 to 2.4 G/cm (for ^{87}Rb, $\Delta=-2\Gamma$, $I=8\ \mathrm{mW/cm^2}$) and seen that the trap depth decreases from 0.27 to 0.13 K. If the trap depth were determined solely by the velocity-dependent forces, it would not change with the field gradient.

The dependence of the trap depth on detuning is more complicated. However, the rapid deterioration of the confining power of the trap at larger detunings can be understood in terms of the Doppler shifts relative to the detuning. For a ^{85}Rb $2\times\Delta F$ collision ($v=5.34$ m/s), the initial Doppler shifts range from 1.16Γ in the (1,0,0) direction to 0.67Γ in the (1,1,1) direction. For a ^{87}Rb $2\times\Delta F$ collision ($v=7.92$ m/s), the corresponding Doppler shifts are 1.72Γ and 0.99Γ. Since these are on the order of 1Γ, we see that a detuning of $\Delta=-1\Gamma$ will be more effective overall than -2Γ in terms of exerting a large initial force. In addition, the damping coefficient (α) is much larger for the smaller detuning.

If the size of the laser beams is increased, keeping all other parameters constant, the trap will rapidly become deeper. For ^{87}Rb, $\Delta=-2\Gamma$, $I=8\ \mathrm{mW/cm^2}$, expanding the beam size from 6.5 to 10 mm, increases the trap depth from 0.26 to 1.3 K. Since larger beams allow atoms to sample larger magnetic fields, the relative importance of velocity- and position-dependent forces will be altered. In addition, larger beams can recapture faster atoms, whose Doppler shifts are better matched by larger detunings. Therefore, the detuning that optimizes trap depth will depend on beam size.

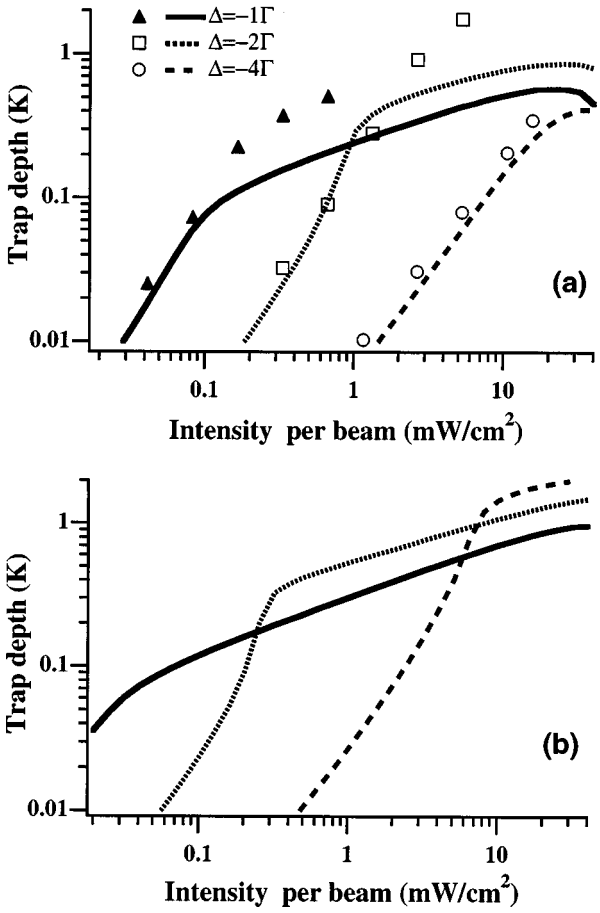

FIG. 3. (a) Dependence of ^{87}Rb trap depth on trap laser intensity for different detunings. The points are the results of the three-dimensional simulations (10% escape fraction) with a beam size ($1/e^2$ diameter) of 6.5 mm, while the continuous curves are the results of the one-dimensional simulations with $z_{\max}=3$ mm. The axial magnetic field gradient is 4.8 G/cm for all cases. Note that the abcissa is intensity is per beam, i.e., (total intensity)/6 for three dimensions. The energy (per atom) corresponding to a $2\times\Delta F$ collision for ^{87}Rb is 328 mK. (b) One-dimensional simulations with $z_{\max}=6$ mm. Other parameters are as in (a).

Our experiments have used a fixed (and relatively small) beam size. If we had used larger beams, the critical intensities for recapture (I_c) would have all been lowered significantly.

In our simulations, we have considered the escape of atoms with a fixed initial velocity at the center of the MOT. This situation is closely related to the loading of a MOT by capturing slow atoms from a room-temperature vapor [24]. In the capture process, an atom enters the trap region with some initial velocity and must be prevented from leaving the trap region in order to be captured. Obviously, the maximum velocity that can be captured will always exceed the maximum velocity that can be recaptured because for capture (recapture), the force acts over the diameter (radius) of the trap. This ability to capture higher velocities, reinforced by the increased weight given to higher speeds in a Maxwell-Boltzmann distribution, will result in an optimum detuning for vapor cell capture that is somewhat larger than the optimum value for recapture following an inelastic collision.

In order to more fully understand the intensity depen-

dence of the trap depth, we have looked at the simpler case of one dimension [36]. An exact expression for the radiative force experienced by a $J=0\rightarrow J'=1$ atom in counterpropagating $\sigma^+-\sigma^-$ laser beams has been derived [37]:

$$F=\hbar k\,\frac{\Gamma}{2}\,\frac{N}{D},$$

where

$$N=\delta\eta[1+4\eta^2]\left(2\,\frac{I}{I_s}\right),$$

$$D=[1+4\eta^2]\left\{Q+\frac{1}{4}\,\frac{I}{I_s}\left[4\epsilon^2+\frac{3}{4}\,\frac{I}{I_s}+4\eta^2\right]\right\}+\frac{1}{4}\left(\frac{I}{I_s}\right)^2\times\left[\epsilon^2+\frac{3}{4}\,\frac{I}{I_s}-3\eta^2\right],$$

$$\epsilon^2=\delta^2+\frac{1}{4}\left(1+\frac{I}{I_s}\right),$$

$$Q=[\epsilon^2-\eta^2]^2+\eta^2,$$

$$\eta=\frac{kv}{\Gamma}+\frac{\mu_B}{\hbar\Gamma}\,\frac{dB}{dz}z.$$

Here, $\delta=\Delta/\Gamma$ is the dimensionless detuning, I is the intensity per beam, I_s is the saturation intensity [$I_s=(2\pi hc\Gamma)/(3\lambda^3)=3.24$ mW/cm^2 for Rb], and μ_B is the Bohr magneton. We have assumed a spatially varying magnetic field $B=(dB/dz)z$ and a g factor of unity for the $J=0\rightarrow J'=1$ transition. The position (z) and velocity (v) dependence is contained in η, the sum of the Doppler and Zeeman shifts. Note that this expression is valid for arbitrary intensity and velocity. We calculate the trap depth for a given $z_{\max}$ (which corresponds to the size of the laser beams) by following atomic trajectories that start at $z=0$. The trap depth is $U=mv_0^2/2$, where v_0 is the maximum initial velocity that can be stopped in the distance $z_{\max}$. The results of such a calculation are shown in Figs. 3(a) and 3(b). In Fig. 3(a), we directly compare the results of the one-dimensional simulations with the more sophisticated three-dimensional ones. The behavior with respect to both intensity and detuning is seen to agree rather well, especially for the smaller trap depths. We note, however, that this comparison is somewhat artificial because we have imposed a cutoff in the one-dimensional simulations that is meant to correspond to the beam size ($1/e^2$ radius) in the three-dimensional simulations. If the problem were truly one dimensional, there would be no cutoff.

We have also used the one-dimensional simulations to examine the effects of beam size. The trap depth for a 6-mm cutoff is shown in Fig. 3(b). These curves are to be compared with the corresponding curves in Fig. 3(a) where a 3-mm cutoff is assumed. As can be seen, not only does the trap depth increase significantly with beam size, but the dependence on detuning also changes. At higher intensities, the trap depth is optimized at a larger detuning for larger beams because of the better match of the higher initial Doppler shift with the detuning.

V. LOSS RATES DUE TO COLLISIONS WITH BACKGROUND GAS

In the previous sections, we have concentrated on the loss of atoms from the trap due to inelastic collisions with other cold trapped atoms. However, an elastic collision with a background gas molecule (at room temperature) will also eject a trapped atom if the energy transfer is sufficiently high. These two different loss mechanisms (cold collisions and background gas collisions) are distinguished by the dependence of their rates on trapped atom density. Cold collisions occur at a rate $\beta n/2$ (per atom) proportional to the trapped density n while γ, the rate (per atom) of background gas collisions is proportional to the background gas density, but independent of the density of trapped atoms. Fitting the temporal decay of trapped atom density allows us to separate these two contributions.

A collision with a background gas molecule can transfer a wide range of energies to the trapped atom, depending on the interatomic potential, the impact parameter, the initial velocity, and the mass ratio. At long range, the energy transfer will decrease with increasing impact parameter, so that for a given trap depth U, we can calculate the maximum impact parameter $b_{\max}$ that will result in ejection. The corresponding cross section for ejection is simply $\sigma=\pi(b_{\max})^2$. For a long-range potential $V(r)=C_n r^{-n}$ (typically $n=6$) and in the impulse approximation, it can be shown [38] that $\sigma\sim U^{-1/n}$. Therefore, as the trap depth is reduced, the background gas collisional loss rate will slowly increase.

The above discussion is completely classical and ignores the wave nature of the collision. For a sufficiently small scattering angle of the incident particle (i.e., sufficiently small energy transfer), it is well known [39,40] that diffraction becomes important and the classical treatment breaks down. This causes the differential cross section (and therefore the total cross section) to level off at a constant value, instead of diverging, as the scattering angle goes to zero. However, this transition from classical to diffractive scattering occurs at energy transfers that are quite low [e.g., 14 mK for N_2 colliding with Rb ($C_6=297\times10^{-60}$ erg cm^6, Ref. [41])] compared to typical MOT depths. Therefore, we would expect to be in the classical regime, where the loss rate is proportional to $U^{-1/n}$. Based on the discussion in Sec. IV, we expect the trap depth to vary between linearly and quadratically with the trap laser intensity I. Therefore the loss rate should have a power-law dependence on I with an exponent between $-1/n$ and $-2/n$, i.e., between $-1/3$ and $-1/6$ for $n=6$. If the trap is shallower than expected (putting us in the diffractive regime), then the loss rate should approach a constant value.

The relative loss rate, γ/γ_0, is plotted as a function of trap intensity for both isotopes and several different detunings in Fig. 4. Here γ_0 is the loss rate (within a given run) for ^{85}Rb at $\Delta=-1\Gamma$ and $I=1.9$ mW/cm^2. This ''standard'' value is used to normalize the loss rate because the pressure is slightly different for each of the several runs needed to obtain the complete data set. Typically, $\gamma_0=0.01$ s^{-1} for a pressure of $\sim10^{-10}$ torr. As can be seen, there is a general trend of increasing γ as we go to smaller trap depth (i.e., lower trap intensity and/or larger detuning). At the largest detuning, the loss rates for both isotopes are seen to increase

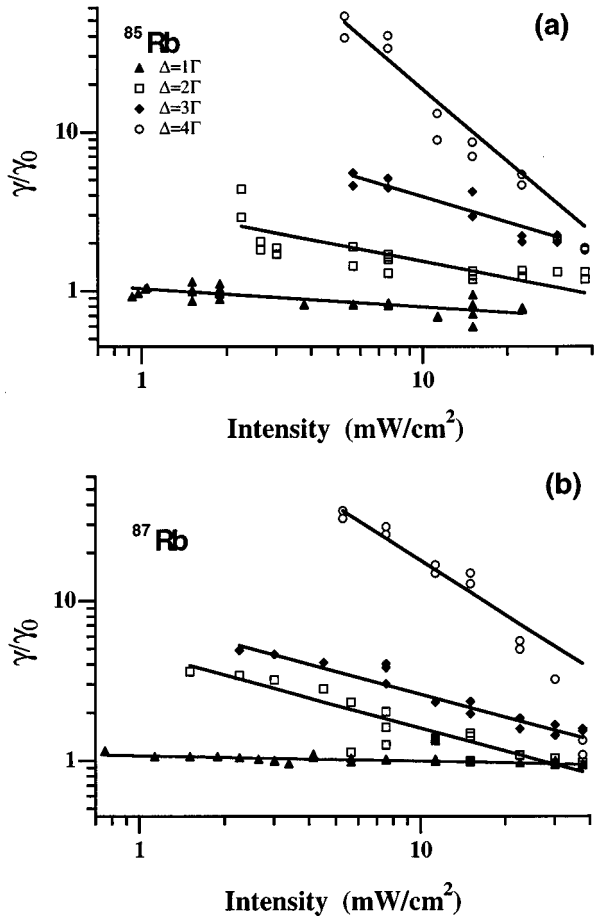

FIG. 4. Normalized background gas collisional loss rate γ/γ_0 vs total trap laser intensity for (a) ^{85}Rb and (b) ^{87}Rb. The different symbols denote different detunings. The straight lines are best-fit power laws to the data with slopes, in order of increasing detuning: (a) -0.12, -0.34, -0.53, -1.50; (b) -0.036, -0.48, -0.47, -1.12.

significantly as the laser intensity is lowered. At the smallest intensity, γ exceeds γ_0 by a factor of ~ 40. This is rather unexpected in light of the above discussion. If there were significant Rb background vapor, ground-excited collisions ($n=3$) with background Rb atoms would eject trapped Rb atoms with an increased cross section [42–44]. However, we have very little Rb background vapor (as evidenced by the absence of trap loading without the atomic beam) and the loss rate is largest at the lowest intensities, where the atomic excitation is minimized. A possible explanation is that for the weakest traps, there is some inherent loss mechanism that does not depend on background gas collisions. We note that a similar behavior (i.e., surprisingly strong dependence of loss rate on trap depth) was reported for a purely magnetic trap [45], but in this case the enhanced loss may have been due to optical pumping caused by scattered light.

VI. SUMMARY

We have investigated the dependence of Rb trap loss collision rates on parameters of the MOT laser trap. In particular, we have varied the trap laser intensity and detuning and found the following behavior. As we increase the intensity (for a fixed detuning), the loss rate decreases sharply as the products of ΔF collisions are recaptured with higher probability. As the detuning is increased, the intensity neccessary for recapture also increases. These trends, as well as the observed differences between ^{85}Rb and ^{87}Rb, are in reasonable agreement with results of numerical simulations of the recapture process. From these simulations, we conclude that, for our conditions, both the velocity-dependent and the spatially dependent forces are important in the recapture process. Above intensities high enough to recapture all ΔF collisions, the loss rate increases with intensity as a result of ground-excited (g-e) collisions. In general, the loss rate is higher for ^{87}Rb (^{85}Rb) when ΔF (g-e) collisions dominate. Finally, we have examined the loss rate due to collisions with room-temperature background gas. Weaker traps (i.e., larger detunings and smaller intensities) have higher loss rates, as anticipated. However, the increase in the loss rate for the weakest traps is much more significant than expected.

There has been significant recent effort directed towards characterizing, understanding, and optimizing MOT's [43,24,30,25,26,36]. The present work is a comprehensive study of the collisional properties of a MOT. As such, it contributes to this overall progress in both a practical sense (i.e., collisional loss and density limitations) and a more fundamental sense (i.e., understanding ultracold collisions and the confining power or depth of a MOT). These results will be relevant to any application using a MOT to prepare a laser-cooled sample. We should emphasize that our measurements (and most of our simulations) have been performed for a fixed diameter of the trap beams. If larger beams are used, while still maintaining the central laser intensity, the influence of ground-state hyperfine-changing collisions (the main process studied here) can be greatly reduced. Also the general dependence of the trap depth on various parameters will change significantly with the size of the laser beams.

ACKNOWLEDGMENTS

This work was supported in part by the Division of Chemical Sciences, Office of Basic Energy Sciences, Office of Energy Research, U.S. Department of Energy. V.S.-V. acknowledges financial support from the INAOE (Mexico).

[1] A. Gallagher and D. E. Pritchard, Phys. Rev. Lett. **63**, 957 (1989).
[2] P. S. Julienne and J. Vigue, Phys. Rev. A **44**, 4464 (1991).
[3] P. S. Julienne, A. M. Smith, and K. Burnett, Adv. At., Mol., Opt. Phys. **30**, 141 (1993).
[4] T. Walker and P. Feng, Adv. At., Mol., Opt. Phys. **34**, 125 (1994).
[5] J. Weiner, Adv. At., Mol., Opt. Phys. **35**, 45 (1995).
[6] K.-A. Suominen, J. Phys. B **29**, 5981 (1996).
[7] D. Sesko, T. Walker, C. Monroe, A. Gallagher, and C. Wie-

man, Phys. Rev. Lett. **63**, 961 (1989).
[8] D. Hoffmann, P. Feng, R. S. Williamson III, and T. Walker, Phys. Rev. Lett. **69**, 753 (1992).
[9] P. Feng, D. Hoffmann, and T. Walker, Phys. Rev. A **47**, R3495 (1993).
[10] D. Hoffmann, P. Feng, and T. Walker, J. Opt. Soc. Am. B **11**, 712 (1994).
[11] M. Peters, D. Hoffmann, J. Tobiason, and T. Walker, Phys. Rev. A **50**, R906 (1993).
[12] P. D. Lett, K. Molmer, S. D. Gensemer, K. Y. N. Tan, A. Kumarakrishnan, C. D. Wallace, and P. L. Gould, J. Phys. B **28**, 65 (1995).
[13] J. Kawanaka, K. Shimizu, J. Takuma, and F. Shimizu, Phys. Rev. A **48**, R883 (1993).
[14] N. W. M. Ritchie, E. R. I. Abraham, Y. Y. Xiao, C. C. Bradley, R. G. Hulet, and P. S. Julienne, Phys. Rev. A **51**, R890 (1995).
[15] N. W. M. Ritchie, E. R. I. Abraham, and R. G. Hulet, Laser Phys. **4**, 1066 (1994).
[16] M. Prentiss, A. Cable, J. E. Bjorkholm, S. Chu, E. L. Raab, and D. E. Pritchard, Opt. Lett. **13**, 452 (1988).
[17] L. Marcassa, V. Bagnato, Y. Wang, C. Tsao, J. Weiner, O. Dulieu, Y. B. Band, and P. S. Julienne, Phys. Rev. A **47**, R4563 (1993).
[18] S.-Q. Shang, Z.-T. Lu, and S. J. Freedman, Phys. Rev. A **50**, R4449 (1994).
[19] R. S. Williamson III and T. Walker, J. Opt. Soc. Am. B **12**, 1393 (1995).
[20] C. D. Wallace, T. P. Dinneen, K. Y. N. Tan, T. T. Grove, and P. L. Gould, Phys. Rev. Lett. **69**, 897 (1992).
[21] C. D. Wallace, V. Sanchez-Villicana, T. P. Dinneen, and P. L. Gould, Phys. Rev. Lett. **74**, 1087 (1995).
[22] E. R. I. Abraham, N. W. M. Ritchie, and R. G. Hulet (private communication).
[23] E. L. Raab, M. Prentiss, A. Cable, S. Chu, and D. E. Pritchard, Phys. Rev. Lett. **59**, 2631 (1987).
[24] K. Lindquist, M. Stevens, and C. Wieman, Phys. Rev. A **46**, 4082 (1992).
[25] M. Drewsen, P. Laurent, A. Nadir, G. Santarelli, A. Clairon, Y. Castin, D. Grison, and C. Salomon, Appl. Phys. B: Lasers Opt. **59**, 283 (1994).
[26] C. G. Townsend, N. H. Edwards, C. J. Cooper, K. P. Zetie, C. J. Foot, A. M. Steane, P. Szriftgiser, H. Perrin, and J. Dalibard, Phys. Rev. A **52**, 1423 (1995).
[27] T. P. Dinneen, C. D. Wallace, and P. L. Gould, Opt. Commun. **92**, 277 (1992).
[28] T. Walker, D. Sesko, and C. Wieman, Phys. Rev. Lett. **64**, 408 (1990).
[29] T. P. Dinneen, C. D. Wallace, K. Y. N. Tan, and P. L. Gould, Opt. Lett. **17**, 1706 (1992).
[30] C. D. Wallace, T. P. Dinneen, K. Y. N. Tan, A. Kumarakrishnan, P. L. Gould, and J. Javanainen, J. Opt. Soc. Am. B **11**, 703 (1994).
[31] T. Walker and D. E. Pritchard, Laser Phys. **4**, 1085 (1994).
[32] V. Sanchez-Villicana, S. D. Gensemer, and P. L. Gould, Phys. Rev. A **54**, R3730 (1996).
[33] J. Dalibard and C. Cohen-Tannoudji, J. Opt. Soc. Am. B **6**, 2023 (1989).
[34] P. J. Ungar, D. S. Weiss, E. Riis, and S. Chu, J. Opt. Soc. Am. B **6**, 2058 (1989).
[35] D. Hoffmann, S. Bali, and T. Walker, Phys. Rev. A **54**, R1030 (1996).
[36] H. Metcalf, J. Opt. Soc. Am. B **6**, 2206 (1989). This work has examined the case of one dimension for a light atom (He*) in the limit of very large detunings ($\gg$ Doppler shifts) and large laser beams (e.g., 8 cm diameter), a situation quite different from the present one.
[37] J. Dalibard, S. Reynaud, and C. Cohen-Tannoudji, J. Phys. B **17**, 4577 (1984).
[38] J. E. Bjorkholm, Phys. Rev. A **38**, 1599 (1988).
[39] R. Helbing and H. Pauly, Z. Phys. **179**, 16 (1964).
[40] R. W. Anderson, J. Chem. Phys. **60**, 2680 (1974).
[41] H. Margenau and N. R. Kestner, *Theory of Intermolecular Forces* (Pergamon Press, New York, 1971).
[42] A. Cable, M. Prentiss, and N. P. Bigelow, Opt. Lett. **15**, 507 (1990).
[43] A. M. Steane, M. Chowdhury, and C. J. Foot, J. Opt. Soc. Am. B **9**, 2142 (1992).
[44] M. H. Anderson, W. Petrich, J. R. Ensher, and E. A. Cornell, Phys. Rev. A **50**, R3597 (1994).
[45] P. A. Willems and K. G. Libbrecht, Phys. Rev. A **51**, 1403 (1995).